A Narrow-Beam Radiometer for Atmospheric Radiation Studies

C. M. R. PLATT

Division of Atmospheric Physics, CSIRO, Aspendale, Victoria, Australia

(Manuscript received 23 March 1971, in revised form 16 August 1971)

ABSTRACT

The design and performance of a narrow-beam radiometer for atmospheric studies are described. It has a beamwidth of 6 mrad and a minimum detectable radiance of 0.0056 mW cm^{-2} sr^{-1} in a 1-Hz output bandwidth. The system incorporates a novel method of comparing flux incident on the aperture against a temperature-stabilized blackbody so that effects due to variations in radiation emitted by or reflected from the chopper blades are eliminated. The radiometer is being applied initially to studies in the 10–12 μm spectral band of the atmospheric "window". Several applications, including the study of water vapor continuum absorption and the emissivity of high layer clouds, are described briefly.

1. Introduction

At the present time increasing emphasis is being placed on problems of atmospheric radiation because of current attempts to model the atmospheric circulation. The Global Atmospheric Research Program (GARP) has set out to study atmospheric systems on an international basis from 1970 onward. The object of atmospheric radiation studies is the measurement of fluxes through atmospheric gases, aerosols and clouds, and from natural surfaces in all important spectral regions as a check on atmospheric radiation models (GARP Publications Series No. 5: Problems of atmospheric radiation in GARP).

The narrow-beam radiometer described here is intended specifically for studies of atmospheric and terrestial radiation. It employs a Golay detector, has a beamwidth of 6 mrad (0.3°) and a minimum detectable radiance of 0.0056 mW cm^{-2} sr^{-1} $Hz^{-\frac{1}{2}}$. It is being used initially to study fluxes in the 10–12 μm region of the atmospheric "window."

The basic design of the radiometer is conventional. Radiation incident on the aperture is compared with radiation from a reference source by mechanical chopping. After detection by the Golay cell, the output alternating voltage is amplified and synchronously rectified with a reference voltage derived from the chopper system. The output voltage is thus proportional to the difference between the source flux and the reference flux. The novelty of the radiometer lies in the design of the reference blackbody and the chopper unit. The reference blackbody actually fills half of the radiometer aperture so that as the chopper blades rotate, they expose either the reference blackbody or the remainder of the aperture (see Fig. 2). The detector "sees" the same area of the chopper blades at all times with no resultant alternating signal. Thus, the alternating signal is a function of the source radiance and reference blackbody radiance only. This system has an obvious advantage over the alternative system in which the reference blackbody flux reaches the detector after reflection from the chopper blades. The full spectral range of detection of the Golay detector (with a potassium bromide window) is from 0.3 to 100 μm and thus any part of this spectral range could be covered by the substitution of suitable filters.

The radiometer and its separate components are described in Section 2 and its calibration and performance given in Section 3. The application of the radiometer to several atmospheric problems is described briefly in Section 4.

2. The radiometer

a. Optical system

The optical system is shown schematically in Fig. 1. Radiation from the chopper aperture (see Section 2b) is focussed initially by a primary spherical mirror of 0.5 m focal length via a plane secondary mirror. A Kodak "IRTRAN 2" meniscus field lens of 25-mm focal length focusses the radiation onto the 3-mm diameter Golay cell window. The $f/25$ tangential aperture of the system ensures that spherical aberration of the image is negligible. A tubular baffle prevents unfocussed aperture radiation from reaching the first focus directly and a 4-mm diameter field stop cuts off radiation which is reflected from the inside wall of the baffle. The filter is a Kodak interference filter having a 1-μm bandwidth centered at 10.7 μm (see Fig. 6).

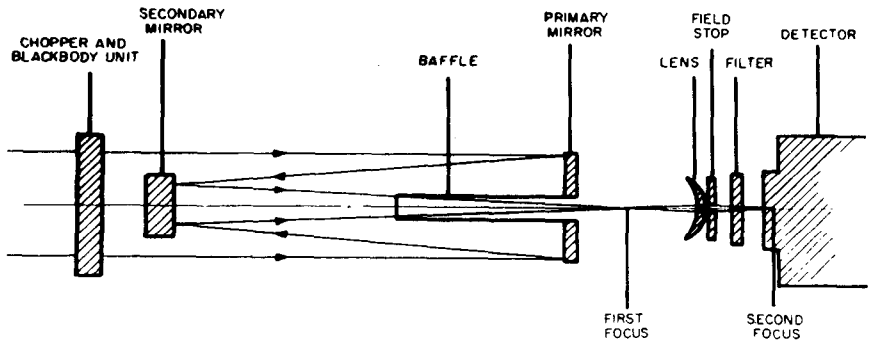

FIG. 1. Schematic plan of radiometer optical system. Dimensions are not to scale.

b. Reference blackbody and chopper system

The system is shown in Fig. 2. The rotating blades are situated behind a grooved aluminum plate and are driven by a small dc motor. The radiometer aperture is formed from two 90° segments cut in alternative quadrants of the grooved plate. The annulus defining the aperture represents the area of the primary mirror which is not concealed by the secondary mirror. When the chopper blades rotate, the *alternating* flux detected at the Golay cell is the difference between the flux from an observed source and that from the reference blackbody.

The grooved plate is maintained at a constant temperature of 40C. It is heated by a coil of constantan wire which is cemented to its front surface, as shown in Fig. 3. Two thermistors are embedded in the plate so as to be just in front of the blackbody grooves (Fig. 3, inset). One thermistor senses the plate temperature and controls the dc current through the heating coil by means of a standard electronic feedback circuit. Temperature control is better than 0.1C under most conditions. The second thermistor provides an independent visual readout of the plate temperature.

A lamp and photocell provide a reference voltage at the chopping frequency of 14 Hz. This voltage is amplified, squared up, and used as the switching voltage for the synchronous detector. Its phase can be varied by moving the lamp and photocell along a groove in the chopper support.

The reference voltage is also used to control the speed of the dc chopper motor. This is necessary because the Golay detector gain varies significantly with signal frequency. Pulses of constant size are generated at the repetition frequency of the reference voltage, and the mean dc level of these pulses controls the current through a power transistor in series with the chopper

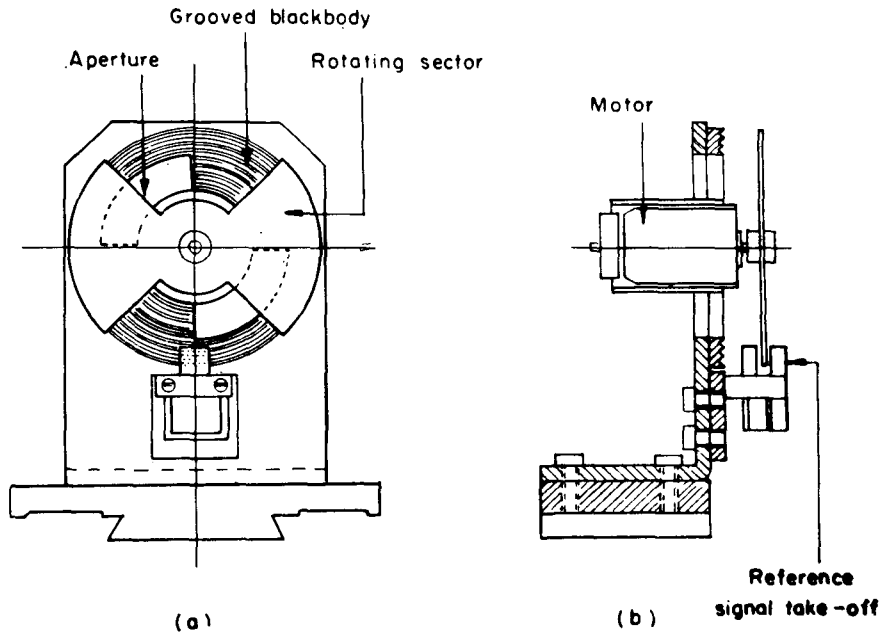

FIG. 2. Diagram of grooved blackbody, radiometer aperture and rotating sector.

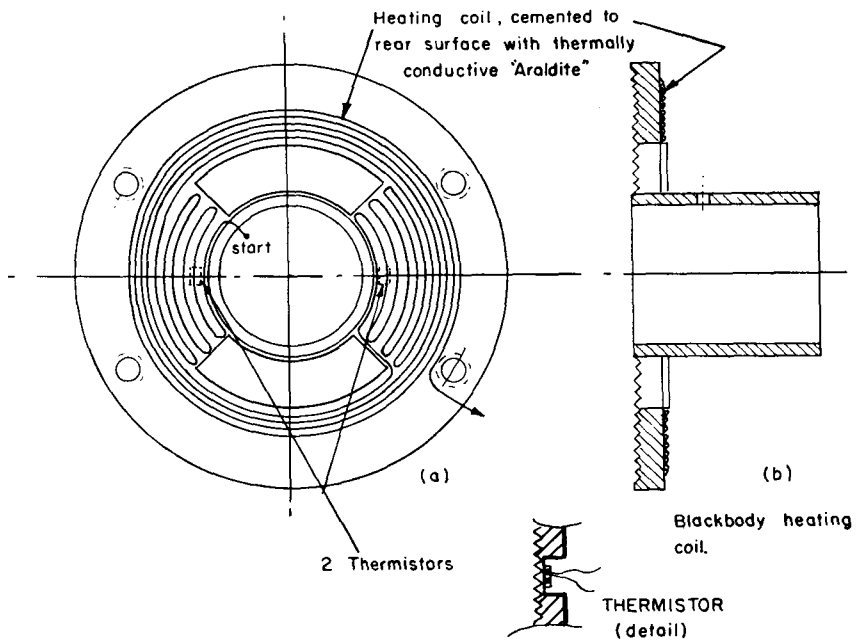

FIG. 3. Detail of heating coil and thermistors for grooved blackbody. Groove dimensions in 3b and inset are schematic only.

motor. The output signal frequency from the Golay detector is thus controlled to better than 0.05 Hz.

c. Detector electronics and layout of components

A block diagram of the electronic circuits is shown in Fig. 4. Transistors are used throughout. The responsivity of the Golay detector is about 10^5 V W^{-1}. Since alternating flux levels incident on the Golay cell are typically in the range of 10^{-10}–10^{-8} W, a following amplifier having a gain of about 1000 gives sufficient output to drive a pen recorder. The amplifier output is synchronously rectified and the output dc voltage is applied to an integrating circuit (1–10 sec time constant) before being displayed on the recorder.

The layout of components (Fig. 5) is designed to be as compact as possible. The Golay detector power supplies, chopper and reference power supplies and blackbody heating control are all external to the radiometer; the remainder of the components and controls are mounted either on or inside the aluminum alloy frame. A white-painted cover fits over the entire frame.

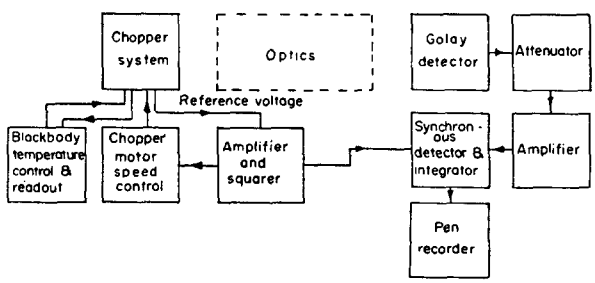

FIG. 4. Block diagram of radiometer electronic circuits.

3. Theory and calibration

a. Theory

The radiative flux on the Golay cell is restricted to wavelengths passed by the IRTRAN filter. It is thus convenient to define an effective blackbody radiance N between the cutoff wavelengths λ_1 and λ_2 of the filter:

$$N(T)=\int_{\lambda_1}^{\lambda_2} F(\lambda)B(\lambda,T)d\lambda, \qquad (1)$$

where $F(\lambda)$ is the filter factor and $B(\lambda,T)$ the Planck function at a wavelength λ and a temperature T.

In the simplest case where the Golay cell receives flux from equal areas (A) and a solid angles ($\delta\omega$) of the aperture and the reference blackbody, respectively, the voltage output (v_S) of the radiometer is given by

$$v_S=\beta A\delta\omega(N_B-N_S), \qquad (2)$$

where N_B is the effective radiance (hereafter simply called the "radiance"), of the reference blackbody, N_S is the radiance of the source observed, and β a system response factor.

In practice, sections of the aperture and blackbody are obscured by the secondary mirror support (see Fig. 5). Also, because of small distortions in the optical system, the effective viewing angle $\delta\omega$ may vary around the aperture. Furthermore, the emissivity (ϵ_1) of the

reference blackbody is less than unity. If the radiometer is viewing a calibration blackbody of radiance N_C and emissivity ϵ_2, a more general expression for $v_C(v_s)$ is

$$\frac{v_C}{\beta A \delta\omega}=(N_B'-N_C')-\gamma_1 N_B'+\gamma_2 N_C'+N_\theta(\gamma_1-\gamma_2), \quad (3)$$

where

$$N_B'=\epsilon_1 N_B+(1-\epsilon_1)N_\theta, \quad N_C'=\epsilon_2 N_C+(1-\epsilon_2)N_\theta,$$

and N_θ is the radiance at ambient temperature. The factors γ_1 and γ_2 define the fractions of the fields of view ($A\delta\omega$) of the reference blackbody and source, respectively, which are at ambient temperature. Substituting for N_B' and N_S' in (3) we find that

$$\frac{v_C}{\beta A \delta\omega}=N_B\epsilon_1(1-\gamma_1) -N_C\epsilon_2(1-\gamma_2)+N_\theta[\epsilon_2(1-\gamma_2)-\epsilon_1(1-\gamma_1)]. \quad (4)$$

The condition for the term containing N_θ to vanish is

$$\epsilon_2(1-\gamma_2)=\epsilon_1(1-\gamma_1)=\kappa(\text{say}). \quad (5)$$

In this case Eq. (4) becomes

$$v_C=S(N_B-N_C), \quad (6)$$

where $S=\beta A\delta\omega\kappa$.

If a source of effective radiance N_S is viewed, then

$$v_S=S\left(N_B-\frac{1}{\epsilon_2}N_S\right). \quad (7)$$

Eliminating S from (6) and (7) we obtain

$$\frac{N_S}{\epsilon_2}=N_B-\frac{v_S}{v_C}(N_B-N_C). \quad (8)$$

Thus, if Eq. (5) is satisfied, the unknown radiance N_s can be determined by quantities which are independent of both the ambient temperature and the emissivity of the reference blackbody. Section 3b describes how this is achieved in practice.

b. Elimination of ambient temperature effects

Experiments were carried out in a controlled temperature room using the blackbody source which is described in Section 3c. The reference blackbody temperature was held at 40C. If Eq. (5) is satisfied it follows that N_B and N_C are equal when v_C is zero [Eq. (6)]. The null point ($v_C=0$) was investigated for various ambient temperatures between 10 and 40C and it was found initially that N_C and N_B were not equal, and that N_C varied with ambient temperature (N_θ), as predicted by Eq. (4). To satisfy (5) it was thus necessary to adjust the optical system in a way which would alter either γ_1 or γ_2. A small piece of metal was placed on one side of the secondary mirror support so that it obscured part of the reference blackbody from the detector. This had the desired effect of reducing the drift in N_C at null, and by careful adjustment, the drift was removed completely. At the same time it was found that N_B was equal to N_C, as predicted by Eq. (6).

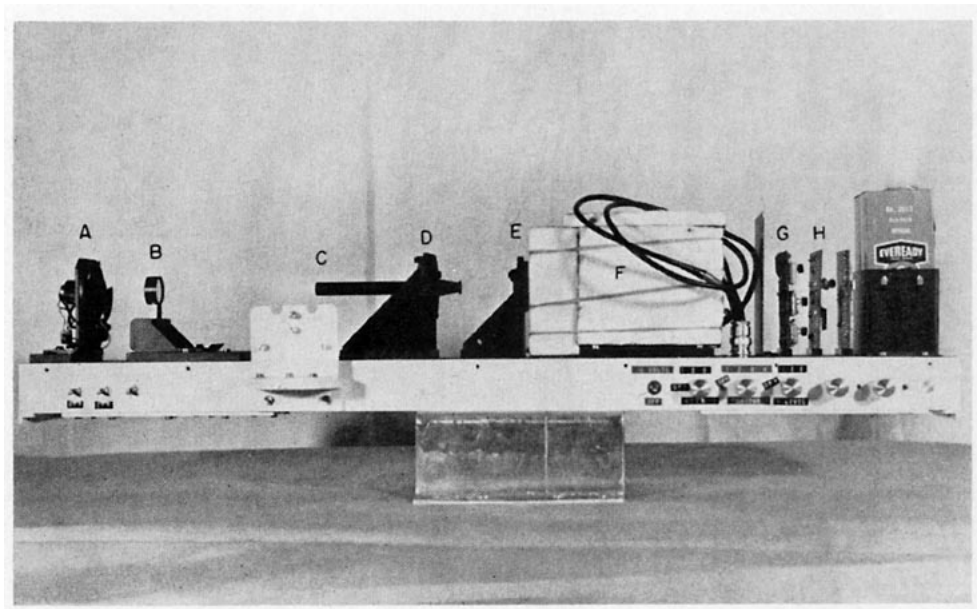

FIG. 5. General view of radiometer: A, chopper and blackbody; B, secondary mirror; C, baffle; D, primary mirror; E, lens and field stop; F, insulated Golay cell; G, amplifier; and H, synchronous detector.

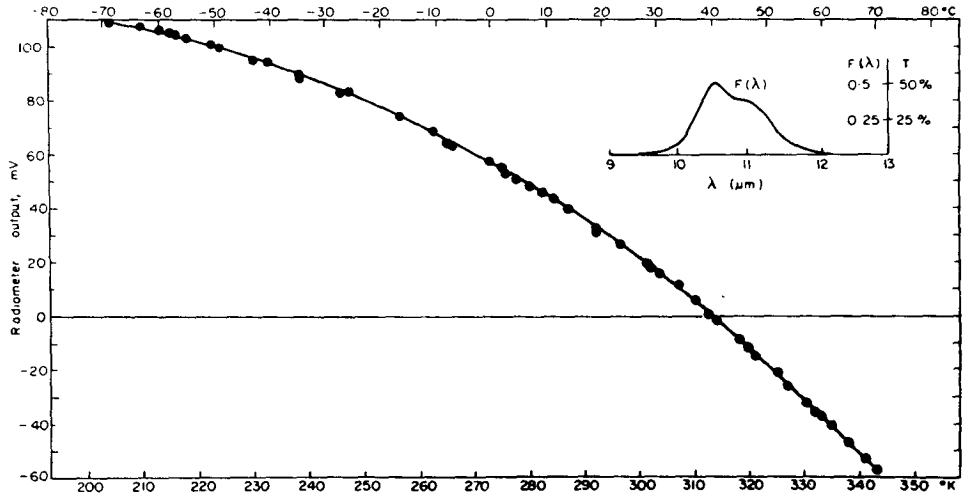

FIG. 6. Theoretical calibration curve (solid line) and experimental points. The filter factor $F(\lambda)$ is shown in inset.

c. Radiometer calibration

The radiometer was calibrated between −70 and +70C. The blackbody source consisted of a cone, semi-angle 15°, painted black on its inside surface. The temperature was varied by circulating water or alcohol around the outside of the cone. The normal emissivity of the blackbody was estimated from figures given for cones of various dimensions by Campanaro and Ricolfi (1967). The emissivity of the black paint used was 0.9 (B. G. Collins, private communication), giving a cone emissivity of 0.984. However, this figure assumes perfectly diffuse reflection from the black paint. Measurements show that at high angles of incidence the reflected radiation would be peaked in the specular direction (B. G. Collins, private communication). Assuming that half the radiation is specularly reflected, the emissivity would be 0.992. The figure assumed for the cone was 0.99±0.004.

Experimental values of v_C plotted against blackbody temperature T are shown in Fig. 6. The full line is the theoretical curve computed from Eq. (1) and fitted to the experimental points. The radiometer transmission factor $F(\lambda)$ in (1) is the product of the spectral transmissivities of the IRTRAN filter, the field lens and the aluminized mirrors. The filter transmission was measured with a Beckman spectrophotometer and the lens transmission was supplied by the manufacturers. Each mirror was assumed to have the theoretical transmission of 0.98, independent of wavelength, from 10–12 μm.

During experimental measurements, the radiometer was calibrated at a single temperature, normally ambient. The observed radiance N_S was then calculated from Eq. (8), using values of N_B and N_C taken from the theoretical curve of N vs T.

d. Linearity and stability

The radiometer has a negative temperature coefficient of gain [β, Eq. (2)] of 1.8% $(°C)^{-1}$ and tests have shown this to be sensibly constant between 5 and 35C ambient. Both interference filter transmittance and amplifier gain have measured temperature coefficients considerably less than this. The only remaining component is the Golay cell which must therefore be responsible for the gain drift. The Golay detector is enclosed in expanded polystyrene to minimize effects of temperature fluctuations and is calibrated frequently during field measurements.

Typical Golay cells are linear to 0.2% for alternating fluxes of less than 10^{-7} W (Hennerich *et al.*, 1966). In the present applications, fluxes never exceed this value. The main amplifier and synchronous detector are linear to better than 0.1%, providing that the input signal voltage to the latter does not approach the reference voltage of 8 V.

e. Minimum detectable radiance

The minimum detectable radiance is here defined as

$$\Delta N = \frac{\Delta v}{S}, \tag{9}$$

where Δv is the rms output voltage noise level. Experimentally, ΔN was found to be 0.0056 mW cm^{-2} sr^{-1} in a 1 Hz output noise bandwidth. The minimum detectable flux ΔF (noise equivalent power) is equal to $A\delta\omega\Delta N$ (Section 3a). Inserting values of $\delta\omega = 2.83\times10^{-5}$ sr and $A = 4$ cm^2, ΔF is found to be 6×10^{-10}W $Hz^{-\frac{1}{2}}$, which is close to the manufacturers' specifications for an "average" Golay cell.

4. Applications

The radiometer is being used at present for several studies in the atmospheric window. These include emission from clear skies at the ground, fluxes in stratocumulus clouds and clear air in the lower tropo-

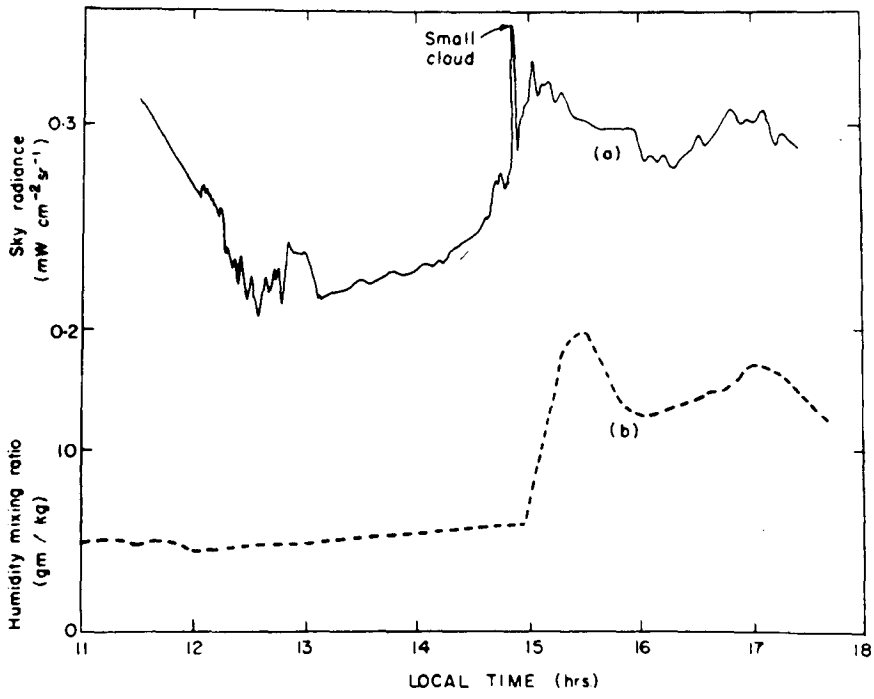

FIG. 7a. Sky radiance at 10–12 μm with the radiometer pointed at 70° from the zenith during passage of a dry cold front. The surface humidity mixing ratio is shown as broken line. (Local time is 10 hr ahead of GMT.)

sphere from an instrumented DC3 aircraft (Platt, 1971), and altocumulus and cirrus fluxes at the ground in conjunction with ruby lidar observations at 0.694 μm (Platt and Gambling, 1971a).

Sample measurements from the three applications are shown in Fig. 7. Fig. 7a illustrates "clear sky" radiance at an angle of 70° from the zenith during the passage of a dry cold front at Aspendale (solid curve). The sky remained cloudless during the measurements except for some very small and scattered cumulus in the frontal zone. The increase in sky radiance at the onset of the cold moist air correlates well with the sudden increase in surface humidity mixing ratio (broken curve). The decrease in radiance up to noon appeared to be associated with the drying out of the air aloft, but the reason for the large "sky noise" between 1200 and 1300 is not known. Many such measurements have been made in the zenith but attempts to compare measured radiance with computed vapor emission indicate a water vapor absorption coefficient of 0.16–0.2 gm^{-1} cm^2, which is higher than that generally accepted by a factor of 2 (Bignell *et al.*, 1963). (The absorptance due to CO_2 was estimated as ~3–5% of the water vapor absorptance.)

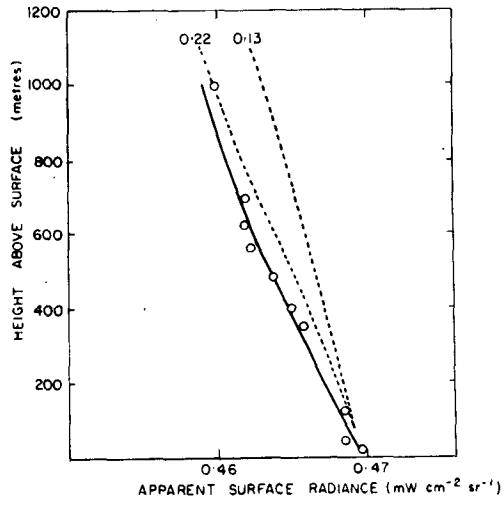

FIG. 7b. Radiance of sea surface and its variation with height. The theoretical variation for logarithmic absorption coefficients of 0.13 and 0.22 gm^{-1} cm^2 is also shown.

Fig. 7b shows the upward radiance in clear air from the sea surface and its variation with height. The decrease in surface radiance with height, which is due mainly to water vapor absorption and re-emission from intervening layers, is again consistent with a continuum absorption coefficient varying from about 0.16–0.35 gm^{-1} cm^2. Recently, Bignell (1970) has reported that the water vapor absorption coefficient is dependent on water vapor pressure, and this could possibly explain the high values of absorption coefficient obtained in both the above studies. Results from these experiments are being examined for this effect.

Fig. 7c illustrated a series of measurements during a combined laser radar (lidar) and radiometric program. The times of lidar shots are marked on the trace as numbers. The program is aimed at obtaining repre-

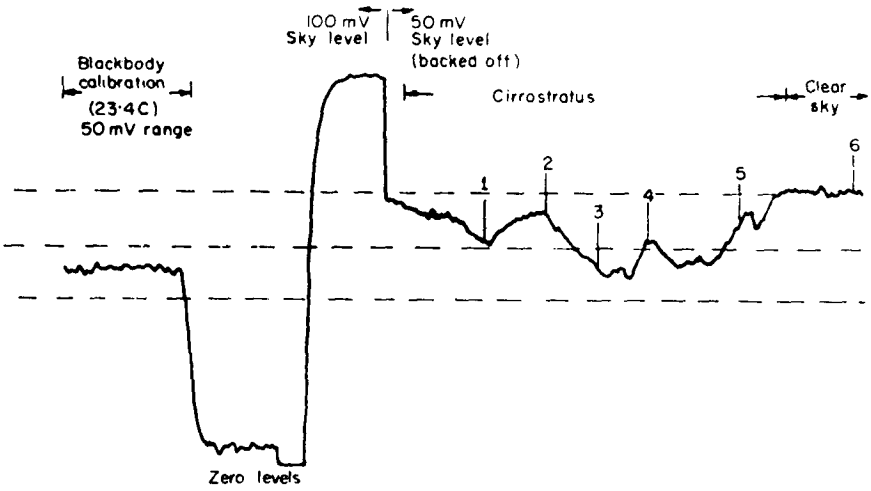

FIG. 7c. Pen recorder output during sequence of measurements on cirrostratus. Lidar firings are indicated by numbers.

sentative values of emissivity at 10–12 μm for both cirriform and altocumulus clouds.

In all these studies the narrow beamwidth of the radiometer has assisted greatly. For instance, small-scale variations in cirrus density (see Fig. 7c) can be detected and correlated with similar variations in both lidar backscatter amplitudes and cloud thicknesses. Similarly, clear-sky fluxes can be measured between small gaps in clouds. In fact, such observations near the *visible* edges of cumulus clouds have shown interesting increases in sky radiance which can be correlated with increases in lidar backscatter (Platt and Gambling, 1971b).

The instrument's ability to measure surface temperatures remotely has been applied to the measurement of sea surface temperatures off the North Queensland Coast from the DC3 aircraft mentioned previously. The measured radiative temperatures agreed with those from bucket measurement to within 0.5C after correction in the usual way for the water emissivity of 0.99. The measurements were made for the Division of Radiophysics, CSIRO, who were investigating anomalous stationary fronts off the coast.

Trial ground-based measurements were also made on a grass surface and a bare patch of soil nearby. On a summer day at noon the grass radiative temperature was 36C, while the bare earth surface was 46C, although the patch was only 6 inches in diameter and surrounded by grass. Thus, the narrow-beam facility of the radiometer has useful application to the study of small-scale features of microclimates within plant communities and over various surfaces. In this context, the replacement of the 1-μm band filter by one covering the 7.5–12 μm region should improve the precision of temperature measurement to better than 0.1C. This spectral band is quite satisfactory for ground-based measurement of surface temperatures. The wider band can be achieved simply by replacing the interference filter by an indium antimonide filter cutting on at 7.5 μm as the IRTRAN$_2$ field lens cuts off at $\sim$12 μm.

5. Conclusions

The novel chopping method described here ensures a stable and reliable source of reference flux. If appropriate adjustments are made (Section 3b), the received signal is independent of both the ambient temperature and the emissivity of the reference blackbody. Frequent calibrations during field measurements eliminate problems due to gain drift in the system (Section 3d).

The Golay cell is ideal for sensitive measurements as it has a very high responsivity and, at the same time, a high detectivity. It can be used in demanding environments, such as an aircraft, without degradation of system noise, provided simple shock mounts are used.

As mentioned in the last section, the narrow beamwidth of the radiometer is very useful, because small patches of cloud, and clear sky between cloud, can be observed. In fact, this facility led to the discovery of the phenomena reported in Platt and Gambling (1971b).

Two future modifications to the radiometer include the elimination of gain drift and the provision of several interchangeable filters for different spectral regions.

REFERENCES

Bignell, K. J. 1970: The water vapor infrared continuum. *Quart. J. Roy. Meteor. Soc.*, **96**, 390–403.

——, F. Saiedy and P. A. Sheppard, 1963: On the atmospheric continuum. *J. Opt. Soc. Amer.*, **53**, 466–479.

Campanaro, P. and T. Ricolfi, 1967: New determination of the total normal emissivity of cylindrical and conical cavities. *J. Opt. Soc. Amer.*, **57**, 48–50.

Hennerich, K., W. Lahmann and W. Witte, 1966: The linearity of Golay detectors. *Infrared Phys.*, **6**, 123–128.

Platt, C. M. R. 1971: Airborne infrared radiance measurements (10 μm-12μm wavelength. *J. Geophys. Res.* (in press).

——, and D. J. Gambling, 1971a: Emissivity of high layer clouds by combined lidar and radiometric techniques. *Quart. J. Roy. Meteor. Soc.*, **97**, 322—325.

——, and D. J. Gambling, 1971b: Laser radar reflexions and downward infrared flux enhancement near small cumulus clouds. *Nature*, **232**, 182–185.